Int. J. Electrochem. Sci., 15 **(2020)** 2677 – 2684, doi: 10.20964/2020.03.61

International Journal of
ELECTROCHEMICAL
SCIENCE
www.electrochemsci.org

Short Communication

Synthesis of CeO_2@S Composite as Cathode Material for in Lithium-Sulfur Batteries

Mingkai Yue[*]

School of Equipment Engineering, Shenyang Ligong University, Shenyang, 110159 China
[*]E-mail: yuemingkaisy@sina.com

Received: 27 November 2019 / *Accepted:* 3 January 2020 / *Published:* 10 February 2020

Rare metal oxides have many appealing characteristics and performance in many aspects, such as photo catalysis and energy storage. In recent decades, traditional metal oxides have been identified as promising cathode host materials for Li-S batteries. The metal oxides could provide chemical adsorption for the soluble polysulfide in the electrolyte. However, there are few works about the employment of rare metal oxides in the lithium-sulfurcould batteries. In our work, metal oxide CeO_2 frameworks are prepared and designed as perfect host materials for the sublimed sulfur. Its unique 3D interconnected frameworks could provide sufficient space for the storage of polysulfide. In addition, the 3D structure is beneficial for the rapid electrons transport.

Keywords: Metal oxides; Energy storage; Li-S battery; Mechanical; Framework.

1. INTRODUCTION

Lithium-sulfur (Li-S) batteries are one of the most promising energy storage devices for the urgent demand of energy consumption [1, 2]. The specific capacity and energy density for Li-S batteries are 1675 mAh g^{-1} and 2600 Wh Kg^{-1}, respectively [3-6]. This is much higher than the traditional lithium-ion batteries [7]. Meanwhile, the sulfur is environment friendly and costless. All of these advantages have drawn much attention of the researchers all over the world [8, 9]. However, there are also some obstacles to inhibit the practical use in the market. The main issues are the poor cycle stability and low specific capacity, which is caused by dissolution of the polysulfide and poor electronic conductivity of sublimed sulfur [10-13].

To deal with these problems, developing more and more superior cathode materials have become hot topic for the researchers on the study of the lithium-sulfur batteries [14]. Because the cathode design plays a key role in the Li-S battery for improving the cycle stability and specific capacity [15]. During the past decades, many kinds of materials have been studied as host materials for

the lithium-sulfur batteries, ranging from carbon materials [16], polymers [17], to metal oxides [18]. At the beginning, various carbon materials were prepared to improve the specific capacity due to their high electronic conductivity, including graphene, carbon nanofibers and carbon nanotubes. After that, polymers are reported to enhance the performance, such as polypyrrole [19] and polythiophene [20]. The conjugated electron in the polymers could efficiently modify the electronic conductivity of the whole cathode materials. Recently, the employment of metal oxides has become a new research direction for the lithium-sulfur batteries.

In this work, we designed hollow CeO_2 frameworks as the host matrix for the sulfur. The as-prepared CeO_2 matrix exhibits interconnected 3D structure, which is beneficial for the rapid electrons transport. Moreover, the big specific surface provide sufficient reaction site for the electrochemical processes. As a result, the CeO_2@S composite cathode shows superior cycle stability and high specific capacity as the electrode for the lithium-sulfur batteries.

2. EXPERIMENTAL

2.1. Preparation of the hollow CeO_2 frameworks

All the reagents were analytical grade and utilized without further purification. First, 2.6 g $CeCl_2 \cdot 6H_2O$ were dissolved in 30 mL distilled water, and named as Mixture A. Then, 1.0 mL oleic acid and 0.5 mL tert-butylamine were mixed in 50 mL methylbenzene, and named as Mixture B. The mixtures A and B were then transferred into a Teflon-lined stainless steel autoclave to heat at 160 °C for 24 h. Finally, the product was collected by centrifugation.

2.2. Preparation of the hollow CeO_2@S composites

The CeO_2@S composites were prepared via heat treatment method at 155℃ for 16 h. The detailed steps are as follows. The sulfur and CeO_2 were mixed with a ratio of 3:1, and ground for 30 min to ensure the uniform distribution. Then, the mixture was transferred into autoclave to heat at 155 ℃ for 16 h. After cooling to room temperature, the products were ground again to make the sample powder like.

2.3. Materials Characterization

The morphologies of the samples were observed by using scanning electron microscopy (SEM, Phenom Pro) and transmission electronic microscopy (TEM, Glacios Cryo). The structure of the samples was analyzed by using X-ray diffraction (XRD, Ultima IV).

2.4. Electrochemical Measurement

Coin 2032 half cells were used for testing the electrochemical performance of the as-prepared CeO_2@S composites. Firstly, the cathode slurry was prepared by mixing the CeO2@S composites, carbon black and PVDF with a mass ratio of 90:5:5. NMP was added to the above mixture and grounded for 20 min. Next, the slurry was uniformly coated on the surface of the Al film and dried at 60℃ for 16 h. After that, the electrode film was punched into circle disc with a diameter of 15 mm. The anode was lithium film. The electrolyte was consisted of 1 M LiTFSI in DOL/DME (1:1). The fabrication of the coin half cells was finished in glove box filled with an Ar atmosphere. Constant discharge and charge profiles were obtained by using battery tester (LANDCT2001A) between 1.5-3.0 V. The electrochemical impedance spectra were obtained on an electrochemical workstation (CHI660E).

3. RESULTS AND DISCUSSION

Figure 1a and b show the SEM images of the pure CeO_2 materials. The pure CeO_2 exhibits 3D interconnected nanostructure. The diameter of the CeO_2 is about 20 nm, which has a framework structure. The unique 3D interconnected frameworks could provide space for the storage of the sulfur and lithium polysulfide. Besides, the 3D framework could promote the transport of electrons during the electrochemical redox reaction [21]. Therefore, the electrical conductivity of the CeO_2@S composites could be greatly improved. As shown in Figure 1c and d, the as-prepared CeO_2@S composites exhibit similar morphology with the pure CeO_2 materials. This confirms the uniform distribution of sulfur in the CeO_2 framework. The uniform distribution can ensure a complete capacity contribution when the CeO_2@S composites are used as cathode materials in lithium-sulfur batteries [22].

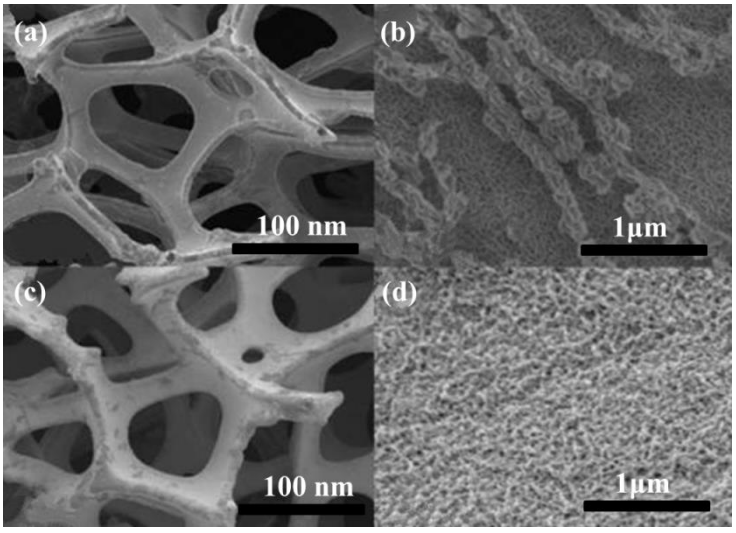

Figure 1. (a) and (b) SEM image of CeO_2, (c) and (d) SEM image of CeO_2@S composites.

Figure 2a shows the HRTEM images of the CeO_2@S composites. It can be seen that the crystal plane of (111) for the CeO_2@S composites, confirming the presence of CeO_2 in the CeO_2@S composites [23]. To further demonstrate the morphology of the CeO_2@S composites, TEM images of the CeO_2@S composites was obtained. As shown in Figure 2b, the interface between CeO_2 and sulfur can be clearly observed. The green line in the Figure 2b represents the boundary of the CeO_2@S composites. Figure 2c shows the corresponding elemental mapping for the CeO_2@S composites. It can be clearly observed that the elements Ce and S are uniformly distributed throughout the whole CeO_2@S composite.

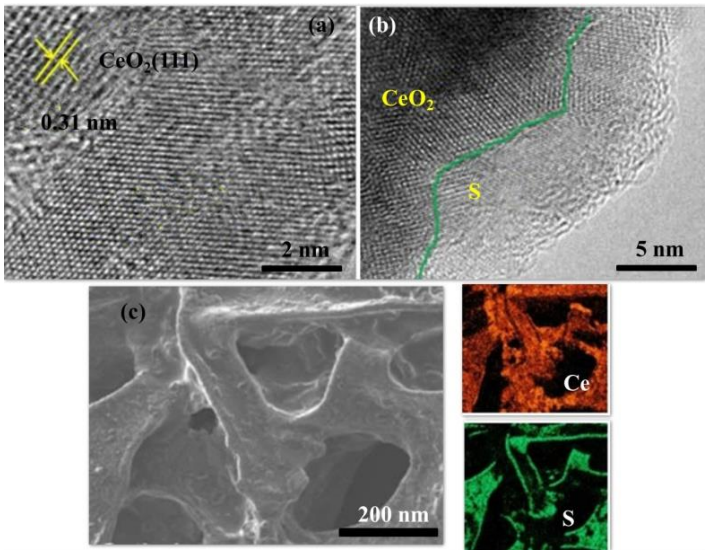

Figure 2. TEM image of CeO_2@S composites showing the (a) lattice spacing and (b) interfaces between the CeO_2 and S (the green line represents the interface). (c) corresponding elemental mapping of Ce and S elements for the CeO_2@S composites.

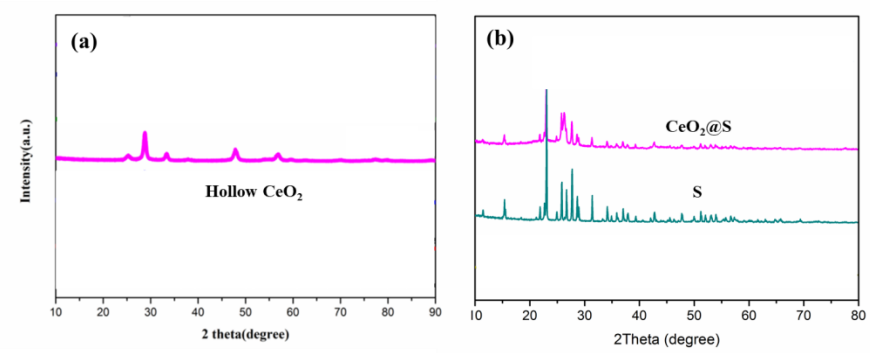

Figure 3. (a) and (b) The XRD patterns of the CeO_2, Sulfur and the CeO_2@S composites.

To confirm the crystal structure of the samples, XRD was conducted with the pure CeO_2, sulfur and CeO_2@S composites. As shown in Figure 3a, the pure CeO_2 shows typical diffraction peaks at 25°, 28°, 32°, 49° and 58°, which are attributed to the different crystal planes of the CeO_2 materials [24].

The XRD pattern of pure sulfur is shown in Figure 2b. The sulfur shows typical diffraction peaks. The as-prepared CeO_2@S composites exhibit the same diffraction peak compared with the pure sulfur, indicating the successful preparation of CeO_2@S composites. However, the peak intensity of the CeO_2@S composites is weaker than that of pure sulfur, which is mainly due to the infusion of sulfur into a hollow CeO_2 framework.

Figure 4a shows the constant discharge and charge curves of the CeO_2@S composites at various current densities from 0.05 C to 1 C. It can be seen that the initial specific capacities of the CeO_2@S composites are 1508 mAh g^{-1}, 1416 mAh g^{-1}, 1356 mAh g^{-1} and 1225 mAh g^{-1} at 0.05 C, 0.1 C, 0.2 C and 0.5 C, respectively. Even at the high rate of 1C, the capacity still reaches at 986 mAh g^{-1}, demonstrating superior electrochemical performance at different current densities. This result also confirms the perfect capacity release of the CeO_2@S composite cathode. Besides, there is no severe polarization for the discharge and charge profiles with the increase of the current densities. This is related to the superior electronic conductivity of the as-prepared CeO_2@S composite cathode [25]. Figure 4b shows the cycle performance of the sublimed sulfur and CeO_2@S composite electrode at 0.1C. The sublimed sulfur electrode suffers from severe capacity fade with an increasing number of cycles. However, for the CeO_2@S composite electrode, the specific capacity value is as high 1008 mAh g^{-1} after 100 cycles at 0.1C, showing excellent cycle stability. The stable cycle performance of the CeO2@S composite cathode is attributed the presence of metal oxide CeO_2 framework, which could efficiently adsorb the soluble polysulfide during the discharging and charging process [26].

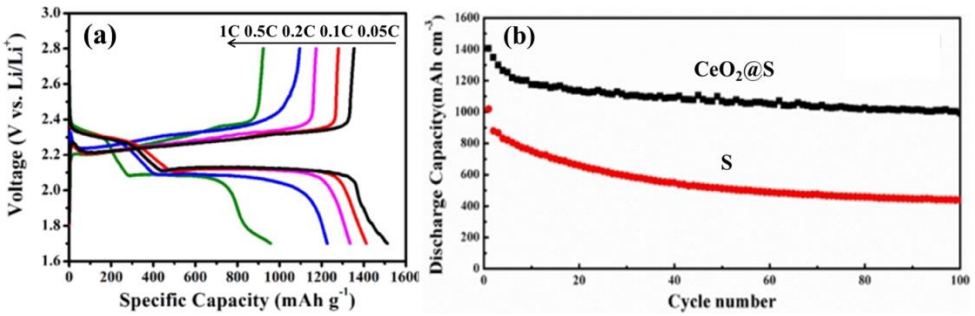

Figure 4. (a) Discharge and charge profiles of the CeO_2@S at different rates. (b) Cycle performance of CeO_2@S composite and sublimed sulfur electrode at 0.1 C.

Furthermore, the long cycle stability of the electrode was tested at 1C for 500 cycles. Evidently, the pure sulfur electrode shows poor cycle performance at high rate for long cycles. The capacity of the pure sulfur electrode is only 201 mAh g^{-1} at 1C after 500 cycles. For the CeO_2@S composite electrode, the specific capacity remains at 756 mAh g^{-1} at 1C after 500 cycles, demonstrating its superior cycle stability. This is attributed to the 3D interconnected framework, which could adsorb the lithium polysulfide and enhance the electronic conductivity at the same time. To confirm the adsorption of the CeO_2 framework, UV–vis spectra was conducted for Li_2S_6 by using carbon black and CeO_2 framework. The strong peak at 420 nm was disappeared after adding the CeO_2 framework. This

indicates that the polysulfide was adsorbed by the hollow CeO_2 framework. However, for the solution of SP, the curve still shows strong peak at 420 nm. This indicates that the adsorption ability is caused by using the metal oxide CeO2 framework while not SP. Therefore, the as-prepared CeO_2@S composites cathode exhibits superior cycle stability at 1C even after 500 cycles [27].

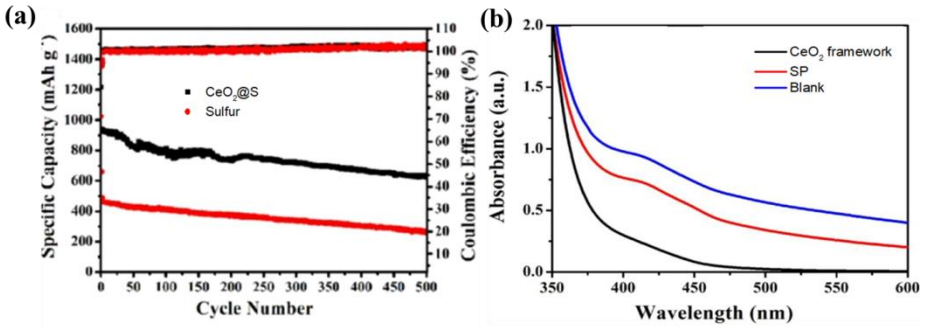

Figure 5. (a) Long cycle stability of the CeO_2@S composites and sulfur electrode at 1C. (b) UV–vis spectra for a blank Li_2S_6 solution and those treated with SP and CeO_2 framework.

Figure 6a shows the rate performance of the CeO_2@S electrode with different sulfur loading of 2.8 and 3.6 mg cm^{-2}. Overall, the as-prepared CeO_2@S composite electrode exhibits high rate performance from 0.1 C to 10 C, which is higher than other reported materials. The CeO_2@S-2.8 displays more superior rate capability than the CeO_2@S-2.8 composite cathode. The electrochemical performance is related to the sulfur loading in the electrode film in the lithium-sulfur batteries. As a result, the low sulfur loading cathode has perfect electrochemical performance. Figure 6b displays the electrochemical impedance spectra of the sublimed sulfur and CeO_2@S composite electrode. The semicircle in the high frequency is corresponding to the charge transfer resistance. The line in the low frequency is related to the lithium-ion transport impedance [28]. It can be clearly seen that the as-prepared CeO_2@S electrode has smaller charge resistance than pure sulfur electrode. This result is consistent with the higher capacity value of the CeO_2@S composite electrode. This result is according with the higher capacity of CeO2@S composite electrode.

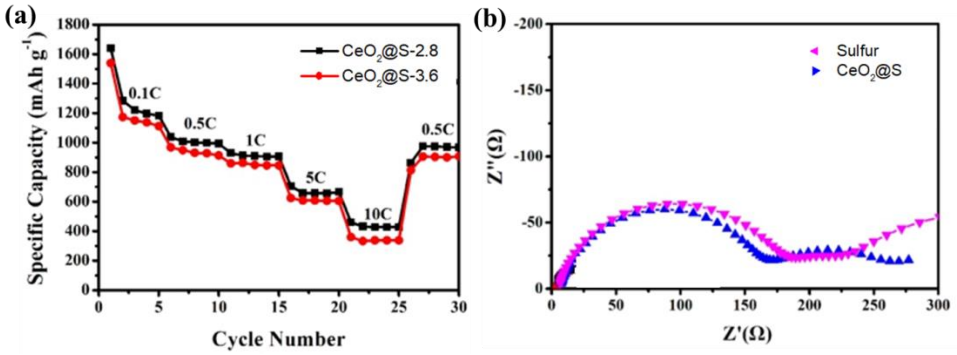

Figure 6. (a) Rate capability for the CeO_2@S electrode. (b) Electrochemical impedance spectra of the CeO_2@S composite and sublimed sulfur electrode.

Table 1 lists the electrochemical performance of the as-prepared CeO_2@S composite cathode with other similar cathode materials for the lithium-sulfur batteries. As shown in Table 1, the capacity value of the CeO_2@S composite cathode remains at 756 mAh g^{-1} at 1 C after 500 cycles, which demonstrates superior cycle stability at high rate for long term cycle performance. However, for other similar cathode materials in the Lithium-sulfur batteries, they all suffer from severe capacity fade with the cycle numbers.

Table 1. Electrochemical performance of the CeO_2@S composite cathode with other reported similar cathode materials for the lithium-sulfur batteries.

Sample	Rate	Cycle Performance	Ref
Ti_4O_7 NRs/S	1 C	580 (300cycles)	29
MnO_2@CMK/S	0.1 C	600 (100 cycles)	30
G@CNT	1 C	755 (200 cycles)	31
CeO_2@S	1 C	756 (500 cycles)	This work

4. CONCLUSIONS

In summary, a rare metal oxide (CeO_2) is successfully prepared via solution method. After that, the CeO_2@S composites are synthesized by a heating method at high temperature. The as-prepared CeO_2@S composites exhibit a hollow framework structure, which can simultaneously enhance the electronic conductivity and adsorb the polysulfide. As a result, the CeO_2@S composites display high specific capacity and long cycle stability at high current density. The initial specific capacity of the CeO_2@S composites is as high as 1416 mAh g^{-1} at 0.1 C. In addition, the specific capacity remains at 756 mAh g^{-1} when tested at 1C for 500 cycles, demonstrating its superior cycling stability. Our work may provide a new direction for designing cathode materials that can be used in lithium-sulfur batteries.

ACKNOWLEDGEMENT
This work is financially supported by the special support of Postdoctoral Research Project of Chongqing (No. XM2017115).

References

1. H. Lin, R. C. Jin, A. L. Wang, S. G. Zhu and H. Z. Li, *Ceram. Int*., 45 (2019) 17996.
2. Y. N. Zheng, Y. K. Yi, M. H. Fan, H. Y. Liu, X. Li, R. Zhang, M. T. Li and Z. A. Qiao, *Energ. Storage Mater*., 23 (2019) 678.
3. W. Z. Bao, Z. Zhang, Y. H. Qu, C. K. Zhou, X. W. Wang and J. Li, *J. Alloy Compd*., 582 (2014) 334.
4. J. W. Guo and M. S. Wu, *Electrochim. Acta*, 327 (2019) 135028.
5. Z. W. Lu, Y. H. Wang, Z. Dai, X. P. Li, C. Y. Zhang, G. Z. Suun, C. S. Gong, X. J. Pan, W. Lan, J. Y. Zhou and E. Q. Xie, *Electrochim. Acta*, 325 (2019) 134920.
6. X. Jiao, P. H. Ji, B. Shang, Q. M. Peng, G. C. Xi, T. B. Zeng, Y. J. Zou and X. B. Hu, *Solid State Ionics*, 344 (2020) 115150.
7. G. F. Chen, J. H. Li, N. Liu, Y. Zhao, J. G. Tao, G. Kalimuldina, Z. Bakenov and Y. G. Zhang,

Electrochim. Acta, 326 (2019) 134968.
8. M. D. Walle, M. Y. Zhang, K. Zeng, Y. J. Li and Y. N. Liu, *Appl. Surf.. Sci*., 497 (2019) 143773.
9. J. Li, L. Zhang, F. R. Qin, B. Hong, Q. Xiang, K. Zhang, J. Fang and Y. Q. Lai, *J. Power Sources*, 442 (2019) 227232.
10. L. You, H. Tang, P. Y. Wang, W. Song, P. Z. Ji, W. J. Xu, C. Q. Feng and J. W. Liu, *J. Alloy Compd*., 798 (2019) 531.
11. W. T. Qi, W. Jiang, F. Xu, J. B. Jia, C. Yang, B. Q. Cao, *Chem. Eng. J*., 382 (2020) 122852.
12. Q. Zhang, X. F. Zhang, M. Li, J. Q. Liu and Y. C. Wu, *Appl. Surf. Sci*., 487 (2019) 452.
13. G. X. Liu, K. Feng, H. T. Cui, J. Li, Y. Y. Liu and M. R. Wang, *Chem. Eng. J*., 381 (2020) 122652.
14. Y. D. Li, Q. Wang, D. G. Zheng, W. P. Li and J. X. Wang, *J. Alloy Compd*., 787 (2019) 982.
15. S. B. Zeng, X. Li, F. Guo, H. Zhong and Y. H. Mai, *Electrochim. Acta*, 320 (2019) 134571.
16. Z. Y. Luo, W. X. Lei, X. Wang, J. N. Pan, Y. Pan and S. Xia, *J. Alloy Compd*., 812 (2020) 152132.
17. S. P. Li, X. Chen, F. Hu, R. Zeng, Y. H. Huang, L. X. Yuan and J. Xie, *Electrochim. Acta*, 304 (2019) 11.
18. Y. S. Liu, Y. L. Bai, X. Liu, C. Ma, X. Y. Wu, X. Wei, Z. Wang, K. X. Wang and J. S. Chen, *Chem. Eng. J*., 378 (2019) 122208.
19. Z. Wang, M. Feng, H. Sun, G. R. Li and Z. W. Chen, *Nano Energ*., 59 (2019) 390.
20. B. E. Li, Z. H. Sun, Y. Zhao, Z. S. Zhang, *Mater. Lett*., 255 (2019) 126529.
21. M. S. Kim, M. S. Kim, V. D. Do, Y. Y. Xia, W. Kim and W. Cho, *J. Power Sources,* 422 (2019) 104.
22. Z, X, Jian, H. L. Li, R. Cao, H. L. Zhou, H. Z. Xu, G. G. Zhao, Y. L. Xing and S. C. Zhang, *Electrochim. Acta*, 319 (2019) 359.
23. H. F. Xu, Y. Z. Shi, S. B. Yang and B. Li, *J. Power Sources*, 430 (2019) 210.
24. P. Liang, L. Zhang, D. Wang, X. L. Man, H. B. Shu, L. Wang, H. Z. Wan, X. Q. Du and H. Wang, *Appl. Surf. Sci*., 489 (2019) 677.
25. J. Pu, Z. H. Shen, J. X. Zheng, W. L. Wu, C. Zhu, Q. W. Zhou, H. G. Zhang and F. Pan, *Nano Energ.*, 37 (2017) 7.
26. P. Q. Guo, D. Q. Liu, Z. J. Liu, X. N. Shang, Q. Liu and D. Y. He, Electrochim. Acta, 256 (2017) 28.
27. Z. Li, S. F. Deng, H. J. Li, H. Z.. Ke, D. L. Zeng, Y. F. Zhang, Y. B. Sun and H. S. Cheng, *J. Power Sources*, 347 (2017) 238.
28. Z. Li, B. Y. Guan, J. T. Zhang and X. W. Lou, *Joule,* 1 (2017) 576.
29. Y. J. Zhang, S. S. Yao, R. Y. Zhuang, K. J. Luan, X. Y. Qian, J. Xiang, X. Q. Shen, T. B. Li, K. S. Xiao and S. B. Qin, *J. Alloys Compd*., 729 (2017) 1136.
30. J. Liu, C. W. Wang, B. Liu, X. Ke, L. Y. Liu, Z. C. Shi, H. Y. Zhang and Z. P. Guo, *Mater. Lett*., 195 (2017) 236.
31. H. W. Wu, Y. Huang, W. C. Zhang, X. Sun, Y. W. Yang, L. Wang and M. Zong, *J. Alloys Compd*., 708 (2017) 743.